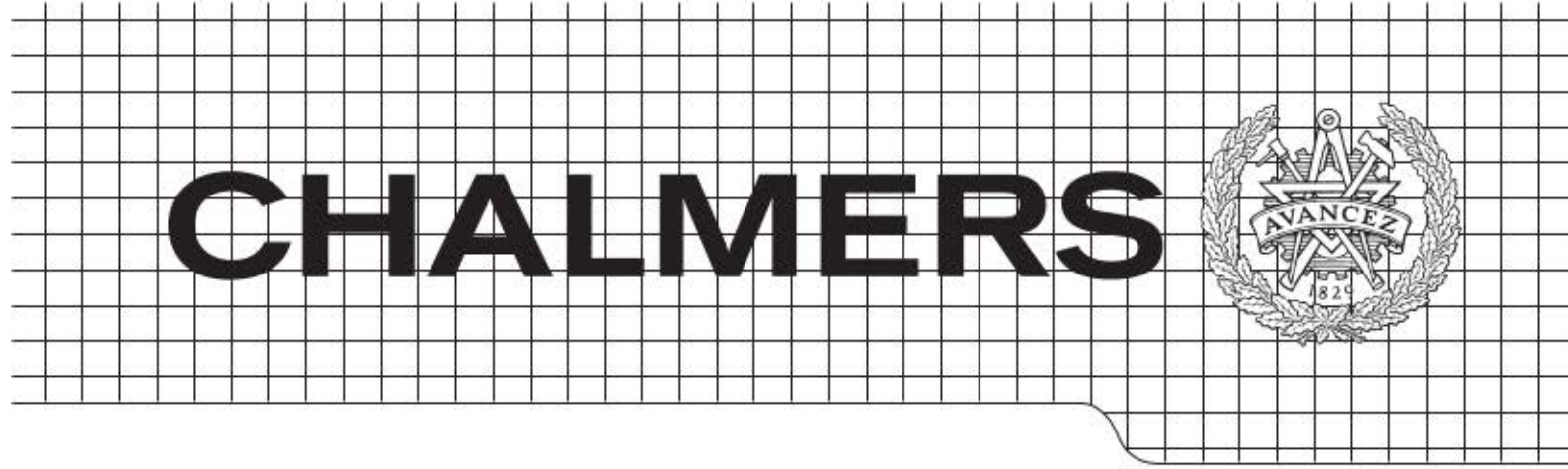

Experimental heat transfer studies with infrared camera

Master's Thesis in Solid and Fluid Mechanics

Carlos Jimenez Sanchez

Department of Applied Mechanics
Division of Fluid Dynamics
Chalmers University of Technology
Göteborg Sweden, 2013

Master's Thesis [2013 : 64]

Master's Thesis 2013:64

Experimental heat transfer studies with infrared camera

Master's Thesis

Carlos Jimenez Sanchez

Department of Applied Mechanics
Division of Fluid Dynamics
Chalmers University of Technology
Göteborg, Sweden, 2013

Experimental heat transfer studies with infrared camera
Master's Thesis
Carlos Jimenez Sanchez

Master's Thesis 2013:64
ISSN: 1652-8557

Department of Applied Mechanics,
Division of Fluid Dynamics
Chalmers University of Technology
Se-412 96 Göteborg, Sweden
Phone +46-(0)31-7721400
Fax: +46-(0)31-180976

Printed at Chalmers Reproservice
Göteborg, Sweden 2013

Carlos Jimenez Sanchez
Master's Thesis
by
Carlos Jimenez Sanchez
jcarlos@student.chalmers.se
Department of Applied Mechanics
Division of Fluid Dynamics
Chalmers University of Technology

Abstract

The master thesis described on this report consists on two experimental heat transfer studies using infrared thermography technology.

The first part, the temperature evolution of two cooled surfaces is studied. Representing the thermal effect suffered by the pistons during the process of injection in diesel engines. The results are compared with CFD simulations and with thermocouple measuremnts that were done previously. This study is useful to understand better the reasons why pistons are damage and to constrast the different methods.

In the second part, the convection heat transfer coefficient inside a linear cascade is studied. This coefficient is measured on a instrumented end-wall, showing the thermal behavior between the vanes and wall interaction. Measuring convection heat transfer coefficient on the endwalls can provide a better understanding of the heat transfer mechanisms in OGVs section. This enables the posibility of optimizing the coolant needed in this section and the material taht can be used for manufacturing OGVs, i.e; composite material are lighter than metal but they have lower melting temperature. Moreover, as in the other experiment the data can be compared with other methods and contrasted with CFD simulations.

Furthermore, another goal of the experiment is to validate this methodology and technique to get this data.

Contents

Part I

Heat transfer study on two cooled surfaces

Chapter 1

Introduction

Nowadays one of the main reasons of engine faillure is due to the wear of the cylinders inside the engine. In mostly of them is shown a crack on the piston head apparently caused by the strong thermal effects suffered during each fuel injection. The experiment reported in this thesis would help to understand how this thermal strong variations affects to this part of the piston, simulating the jet conditions and the relative position between the jet and the piston surface during the transient. The data obtained from this experiment was compared with the simulation and with another experiment carried out in a different method.

1.1 Main objective

The main objective of this experiment is the thermal study of two different heated surfaces with the help of an infrared thermal camera. For this case it will be studied the thermal gradient effects caused by single jet impingement on these two heated surfaces, in differents position. In order to see which are the thermal effects and the heat transfer all along the two studied targets several pictures were obtained with the infrared camera. The aim of this is to understand how the material reacts to the jet, in terms of heat transfer, and figure out how it can affect to the piston.

1.2 Case simplification

As it is known, the fuel injection inside the diesel engines is almost instantaneous, which means that the piston travels at a high speeds during the injection. Due to this high velocity of the piston, the jet of fuel does not always impact in the same position above the pistons head. In fact, the

angle of the injection changes respect to the piston for each time fraction. See figure 1.1

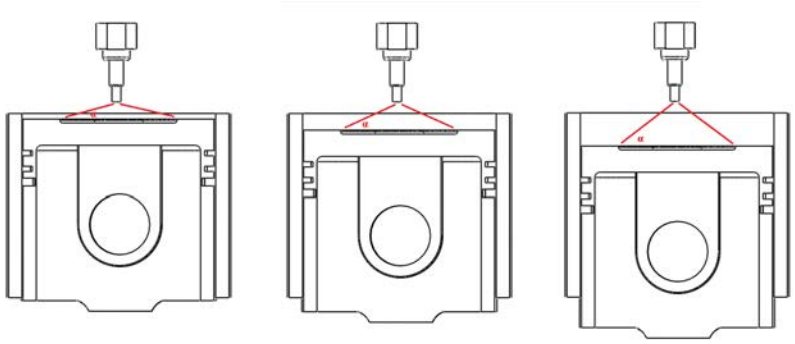

Figure 1.1: Variation of the injection angle

In order to represent these angle variations one of the targets is tilted several degrees trying to represent what happens inside the engine. To capture this rapid event the camera is setup at a high frame rate.

Obviously, it is impossible to reproduce the injection conditions from a diesel engine because of the high pressure and temperature. For all these reasons the case is highly simplified but keeping always in mind the reference case. The main purpose is to study the thermal effects of a pulse jet approaching a wall and extrapolate the data obtained into the real case. Instead of a fuel spray, a high pressure air jet is used to simulate the injection.

Regarding to the two different targets that are studied, the first one is a flat and circular surface and the second one is a ninety degrees surface with circular base. The two of them have 60 mm of diameter and are made of aluminium. In both cases the targets are painted with a black special coating, which has a very high emissivity coefficient (around 0.973) and low angle dependence in order to provide the needed conditions to the infrared camera.

For the targets heating, two cilindric heaters are used. These heaters are placed inside the targets crossing the whole section to provide an uniform temperature all along the studied surface. With the help of a termocouple placed next to the heaters and a PID heat source, the temperature is settled and monitorized to 150 celsius degrees in both of the cases during the experiment.

Chapter 2

Theoretical background

Every experiment is based on theoretical knowledges. In this case, as in the previous one, the study is about heat trasnfer and heat transfer mechanisms. The main difference from the other experiment is that we focus on the transient heat transfer instead of the steady state, taking into account the interval of time. This chapter tries to expose which are these background knowledges and to clarify the assumptions done in this experiment.

Thermal conduction is caused by the temperature gradient between the particules, with stronger effect inside solids. Atoms and molecules with higher levels of energy (heat) transfer some of their energy to the less energetic neighbors particles by vibration. This heat mechanism strongly depends on the material, each material has different conduction characteristics, from the way how they transfer the energy between particles (isotropic or anisotropic) to how easily they transfer the energy (diffusion parameter). From Fouriers law we obtain the heat conduction equation:

$$\rho c_p \frac{\partial T}{\partial t} = \nabla(k\nabla T) + \dot{q} \tag{2.1}$$

where ρ is material density, c_p is heat capacity, T is temperature, t time, k the material conductivity and $\dot{q}$ heat generation. For steady states the term on the left becomes zero as it is seen in the second experiment, not in this case (see part 2, theoretical background).

This general equation can be simplifeid taking into account some considerations:

- No internal heat generation

$$\dot{q} = 0 \rightsquigarrow \rho c_p \frac{\partial T}{\partial t} = \nabla(k \nabla T) \tag{2.2}$$

- 1D case

$$\rho c_p \frac{\partial T}{\partial t} = \frac{\partial}{\partial x} k(\frac{\partial T}{\partial x}) \tag{2.3}$$

- Constant material properties in the range of temperatures studied: ρ, c_p and k are constant

$$\frac{\partial T}{\partial t} = \frac{k}{\rho c_p} \frac{\partial^2 T}{\partial x^2} \tag{2.4}$$

Finally we obtained the heat conduction equation for this case:

$$\frac{\partial T}{\partial t} = \alpha \frac{\partial^2 T}{\partial x^2} \tag{2.5}$$

where α is the material difusion.

Chapter 3

Setup for measurents

This chapter describes in more detail the preparation and the procedures to carry out the experiment, such as the elements involved, the previous infrared camera setups, the jet and camera syncronization or the targets painting. It also shows all the steps followed during the whole process.

3.1 The jet

In order to simulate the fuel injection, a gas jet is generated by a modified diesel DI injector. The manufactured jet has a nozzle of 1mm diameter and 6mm long hole sealed by a needle with spherical tip.

The nozzle of the jet is placed at 40 mm from the warmed targets. Synthetic air is used as the jet fluid. Fluid conditions on the top of the nozzle are 10 bar of pressure and 20 Celsius degrees of temperature. The jet is shot directly towards the objectives under atmospheric conditions (15^{o}C). One single supersonic shot lasts 5 milliseconds in total and is fully developed after the first millisecond approximately.

The average velocity of the jet is 40m/s which means that the jet took around 1ms to reach the tagets. Previous PIV (Particle Image Velocimetry) studies shown that the jet has such a small desviation when impacting straight in the middle of the target, so many shots are recorded to average the results.

3.2 Targets

For the purpose of representing the different relative positions between the fuel injection and the head of the piston, inside a diesel engine, two targets are used.

The first of them is completely flat, in order to simulate the several angles of the jet impact. The target is made of aluminium, which is the same material as in real pistons. Circular, 60 mm of diameter and 15 mm of thickness. The piece has two holes accross the section to place the two heaters and a termocouple is placed next to the impact surface to control the temperature. See figure 3.1

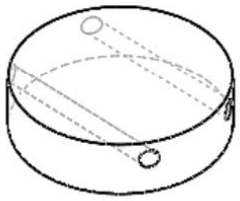

Figure 3.1: Flat target draw

Regarding to the other target, it is used to represent the jet impact above the top part of the head piston, the corner. The target has a ninety degrees shape with a circular base of 60mm. It is also made of aluminium, has two holes to place the heaters and a termocouple to follow the temperature. See figure 3.2

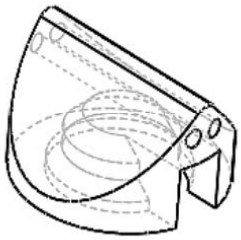

Figure 3.2: Ninety degrees target draw

For the flat target a total of 4 different position are studied , representing the first time after the injecton until the latest one, respectively:

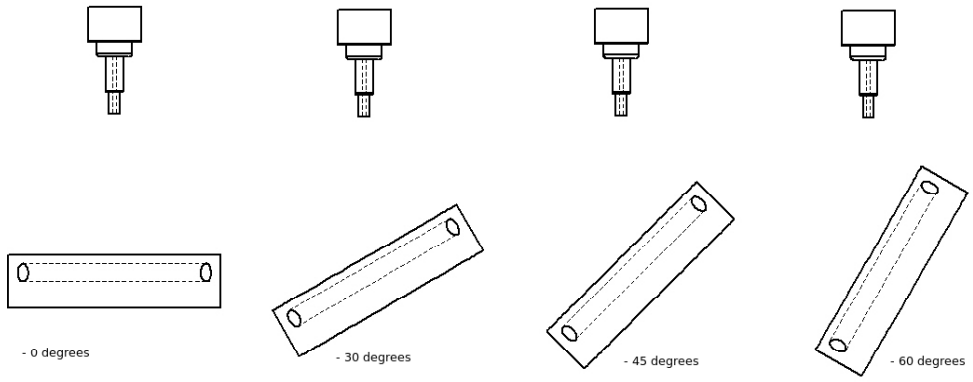

Figure 3.3: Different flat cases

Two different positions were studied from the ninety degrees target, with 90 degrees diffence between each one: Figures

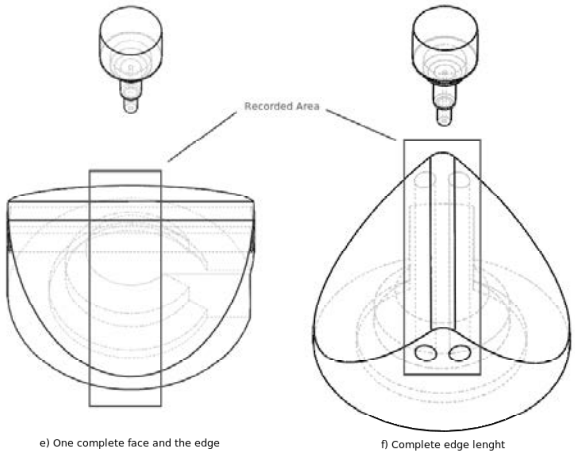

Figure 3.4: Different ninety cases

3.3 Painting treatment

In order to maximize the camera precision it is better to point the camera to a black body radiation surface. In our case, both targets are made of aluminium which has very low emissivity factor. For this reason it is needed to make a paint treatment to the targets to increase them emissivity and reach, as far as possible, the blackbody emissivity properties.

The paint used is the Nextel Vetel-Coating 811-21 from Mankiewicz Gebr. & Co, the main properties that make this coating usefull are the high emissivity value of 0.973, which is almost the same of the blackbodies (1) and the independence of the emissivity with the angle, which is very important in our case due to the different angles studied for the flat target. Table 3.1 shows the specifications of this coating.

Physical Property	Value	Comment
Total emissivity	973	Constant for our temperature range
Maximum angle for constant emissivity	30 deg	60º for 1% drop
Thermal conductivity	0.2 W/mK	Constant for our temperature range

Table 3.1: Nextel Vetel-Coating 811-21 specifications.[2]

During the painting treatment several layers of paint are applied on the targets, four in total. Between each layer of paint is needed to wait until the paint is dry, the heaters are used to accelerate this paint drying. Once the experiment is done the coating thickness is measured to take into account the isolation factor due to its low thermal conductivity.

Figure 3.5: Flat and ninety degrees target after the painting treatment

Once the surfaces of the targets are painted, we need to mark the center of the target to know where exactly the camera is pointing. To do this a silver point marker is used. The point is that the silver ink has low emissivity

therefore, high reflectivity compared to the black coating, this allows us to see a big difference between them when looking through the infrared camera. One of the problems of this silver marking is that some information is lost during the experiment, but in the post processing part of the experiment this problem is solved.

3.4 Camera setups

In this chapter is described the infrared camera setups done to measure, as accurate as possible, the experimental data. The IR-Camera camera used is a MWIR Phoenix Camera System with a 320x256 resolution. The specifications can be seen in the table below.

Manufacturer	Flir Systems Inc.
Model	Phoenix MWIR Camera System
Detector type	Indium Antimonide
Detector spectral response	1 µm - 5.4 µm
Filtered spectral response	3 µm - 5 µm
Format (pixel number, HxV)	320 x 256
Detector pitch	30 µm
Detector cooling	Stirling cycle
Detector temperature	77 K
Dynamic range	14 bit
Noise equivalent temperature difference (sensitivity)	25 mK
Minimum window	2 rows x 4 columns
Integration mode	Snapshot
Max frame rate full window	122 Hz.
Max frame rate minimum window	13.6 kHz
Integration time	9 µs - 16.6 ms
Output	Composite video / digital image / RS.232 camera control
Input	Sync (arm/trigger) / RS 232 camera control
Optics	25 mm f/2.3 MWIR / Janos Technology

Table 3.2: Camera Specifications.[7]

3.4.1 Windowing and basic configurations

The first step is to set the integration time of the camera and the gain levels. The IR-Camera reads the temperature as a concrete number of counts, from 0 to a total of 16000. In order to work with a high camera precision, the integration time has to be set around this maximum of counts. In this case due to the high range of temperatures the number of counts must be as maximum 75 per cent of the total to avoid the camera saturation. To do this, a uniform heated cupper cone is used. That cone device is heated up 5 C higher than the maximum temperature that is going to be achieved during the experiment. Then pointing at the cone (hot source) with the thermal camera and looking the number of counts, the integration time is set.

Another important camera setup for this experiment is the camera's window size configuration. In this case due to the fast data collection,the size of the camera's window (the number of pixels that the camera uses during the acquiring process) needs to be reduced. The maximum size, to be able to work at such high speeds, is 64x14 pixels instead of 320x256 as usual. Obviously the information is lower when reducing the size of the window but it is still high enough for the purpose of this experiment.

3.4.2 Non-uniformity correction and calibration

The infrared detectors of the thermal camera vary in their individual response to photon energy, this variation is known as detector non-uniformity. To avoid this non-uniformity, some type of corrections needs to be performed. The best option is to apply a two point or gain and offset correction. This process is done by measuring the output voltage of each detector element at two temperatures points, assigned as hot and cold source. These two sources should bound the temperature range of the scene of interest and be at least 10 below the saturation level and 10 above the bottom rail respectively.[citar manual]

In this case a cupper cone device, named in the previous section, is used to provide the two sources. This device consists in an isolated cupper plate, traeted with the same coating as the targets, supported by a conical structure. The aim of this tool is to garantee a uniform temperature surface. This device is heated up to 50 degrees for the cold source and 155 for the hot source.

Next step is to generate a 4 grade polynom to translate the counts readed by the camera to temperature values. These process is called calibration. It consists into read five different temperatures with the camera, inside the range of the experiment boundaries. In this case from 140 degrees until 153 with steps of 3 degrees. The conic device is used as well in this process.

Once the five values are taken the RDcal software is used to generate the calibration polynomial, note that the emissivity value from the surface has to be known, which is 0.973 because of the black coating.

3.4.3 Jet and camera syncronization

For each case the thermal camera records 20 shots. Each shot lasts 5 miliseconds and the elapse time between shots is 4 seconds. During every shot the camera takes 15 pictures. Every half a milisecond to see the whole injection and part of the recovery. It is necesary to syncronize the jet and the camera acquisition to ensure that the pictures are always taken when the jet starts. One pulse signal generator sends a positive burst signal to the camera for the acquiring process. Using this signal as a clock, another pulse signal generator tells the jet when to start the injection and its lenght, with a negative pulse. See figure 3.6.

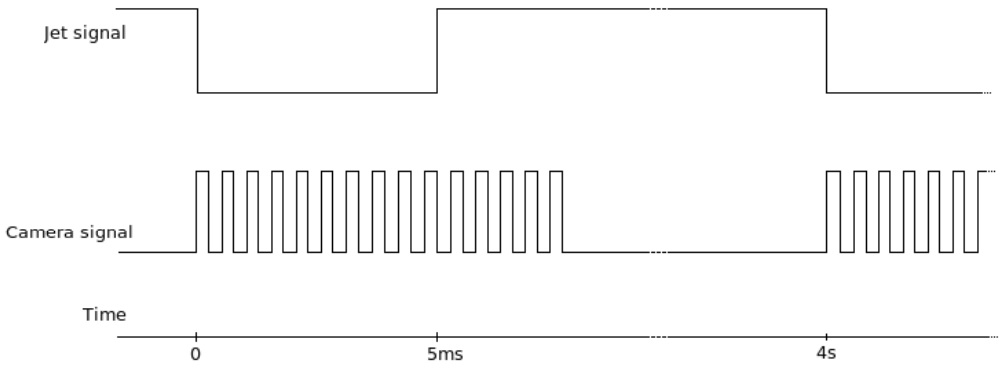

Figure 3.6: Jet and camera imput signals

The external signal option from the Phoenix User's software must be selected so the camera can read the signal and know when to start the trigger.

Chapter 4

Results

This chapter shows the post process data method and the results obtained for each case. It is also compared the thermal camera results with the simulation and the thermocouples methods.

4.1 Post processing

After the asquisicion of the pictures with the infrared camera, the collected data must be transformed into useful information. Each picture is stored as a matrix of 14x64 numbers (see windowing section 3.5.1), each number represents the temperature of each pixel. The software used to handle the experimental data is Matlab.

First of all, the calibration polynomial is used to translate counts to temperature in Celsius. Next step is to filter the images in order to remove the possible bad pixels and delete the areas of non interest such as the outside of the target. In this filtering process, the maximum and minimun expected temperature of the target during the experiment are fixed, so if there is any pixel with higher or lower temperature it is automatically removed. It can be done as many times as needed to have a more accurate temperature scale. Figure 4.1 and 4.2 represents this filtering process.

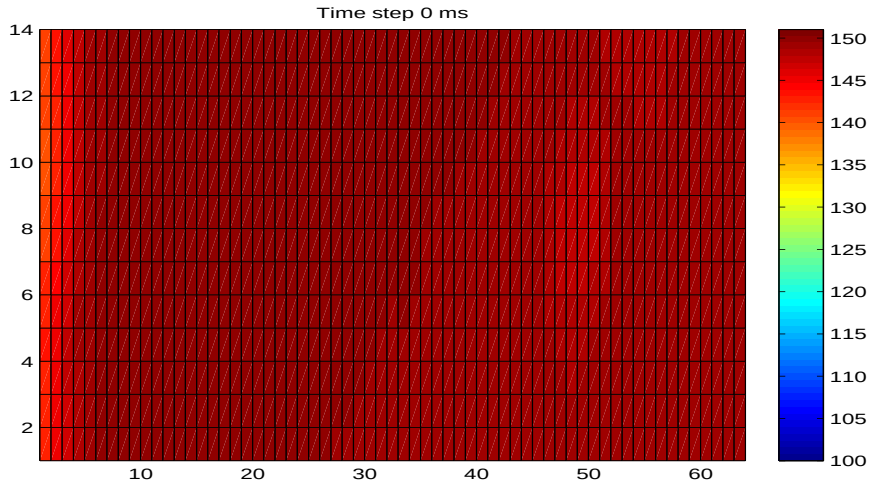

Figure 4.1: Zero degrees case before filtering

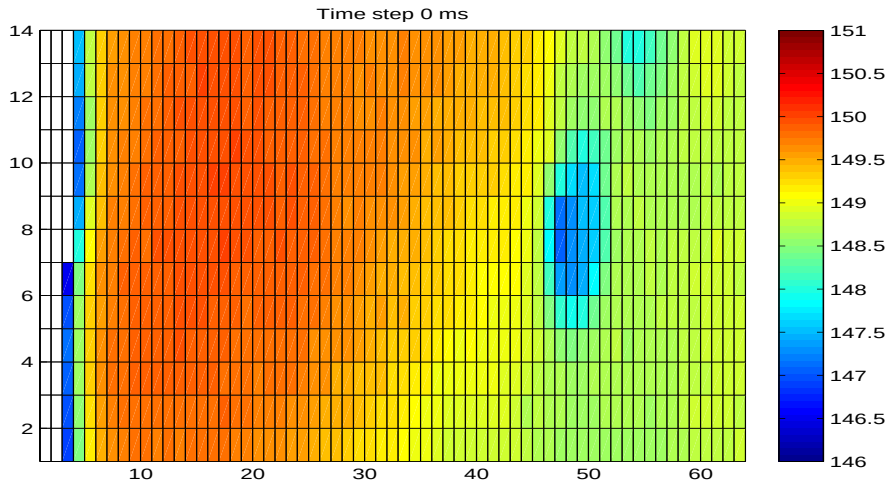

Figure 4.2: Zero degrees case after filtering

Once filtered the pictures, what follows is to assign to each pixel of the image a specific x and y coordinates setting the center of the target as the origin. Looking at the image it is clearly easy to distinguish the dot, which is in the center of the target. Next step is to define where is the edge of the target, as it has been seen in the picture above, there are some pixels with a very different temperature on the left side. This is because these pixels represent the outside of the target, so the first good pixel found (a pixel with

an approximately same temperature than the whole target) is set as the limit of the target so the radius is fixed. Afterwards, knowing the dot coordinates and the target radius in the image, all the pixels are provided with an x and y coordinate in reference to the center.

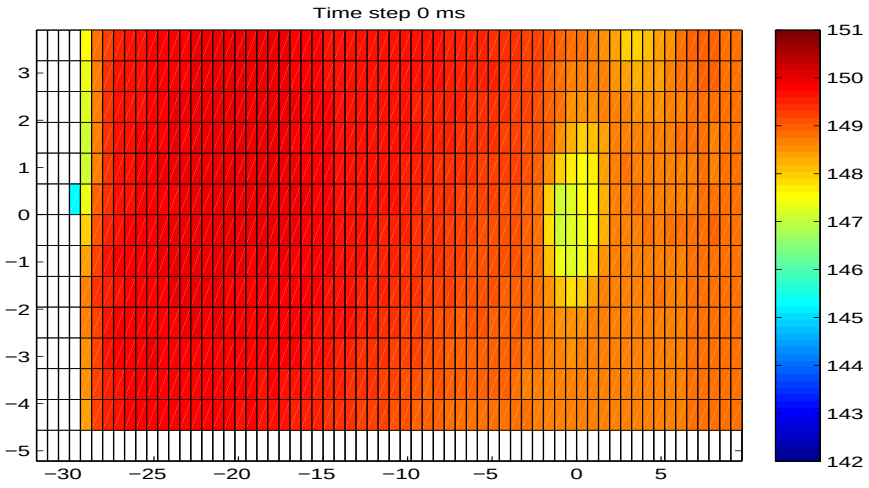

Figure 4.3: Zero degrees case after placing coordinates

The jet does not impact the target after the first milisecond, so for representing the temperature results,the average of the first two frames of each shot are taken as the reference. Then from this reference the temperature variation of pictures is calculated and ploted with one milisecond difference, from the first (when the jet impacts the target) until the 5th milisecond (when the jet is supossed to be ended). In each it can be seen how the jet cools down the surface depending on the angle variation.

Last step made is to analize single rows of the pictures in order to see the thermal variation in the target surfaces produced by the jet cooling effect. In this part, the average of the 20 shots, acquired for each case, is used to represent such thermal variation. Figure 4.4 show this temperature decreasing for the zero degrees zoom in case.

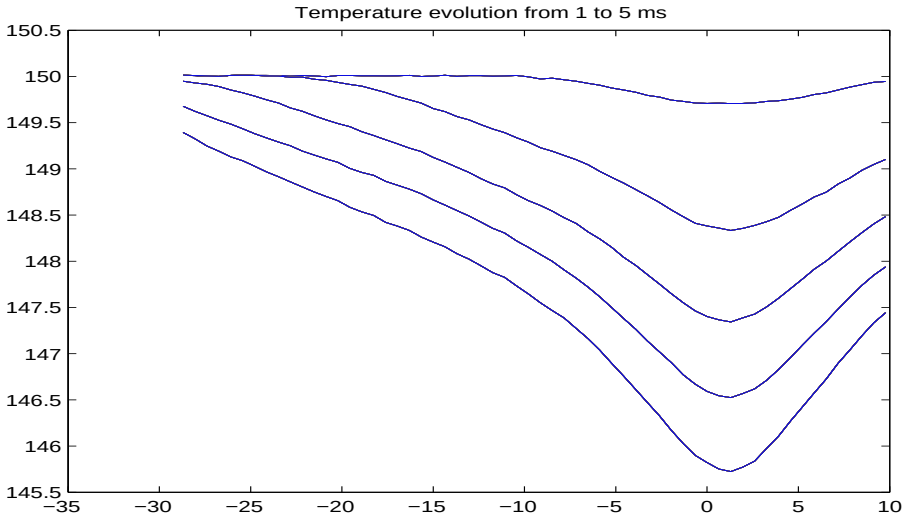

Figure 4.4: zero degrees zoom in case

Zero degrees zoom in case

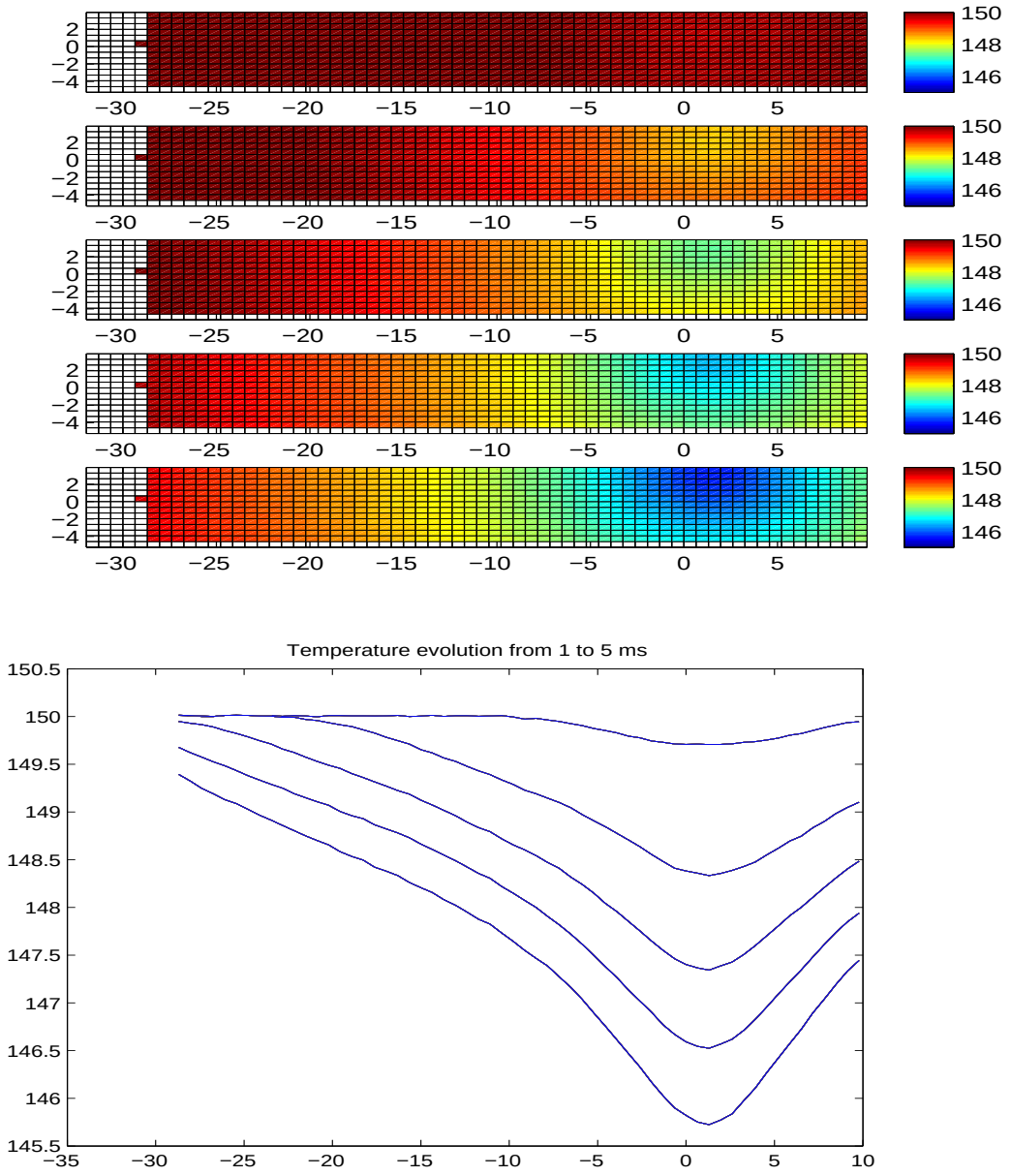

Figure 4.5: zero degrees zoom in case

Zero degrees zoom out case

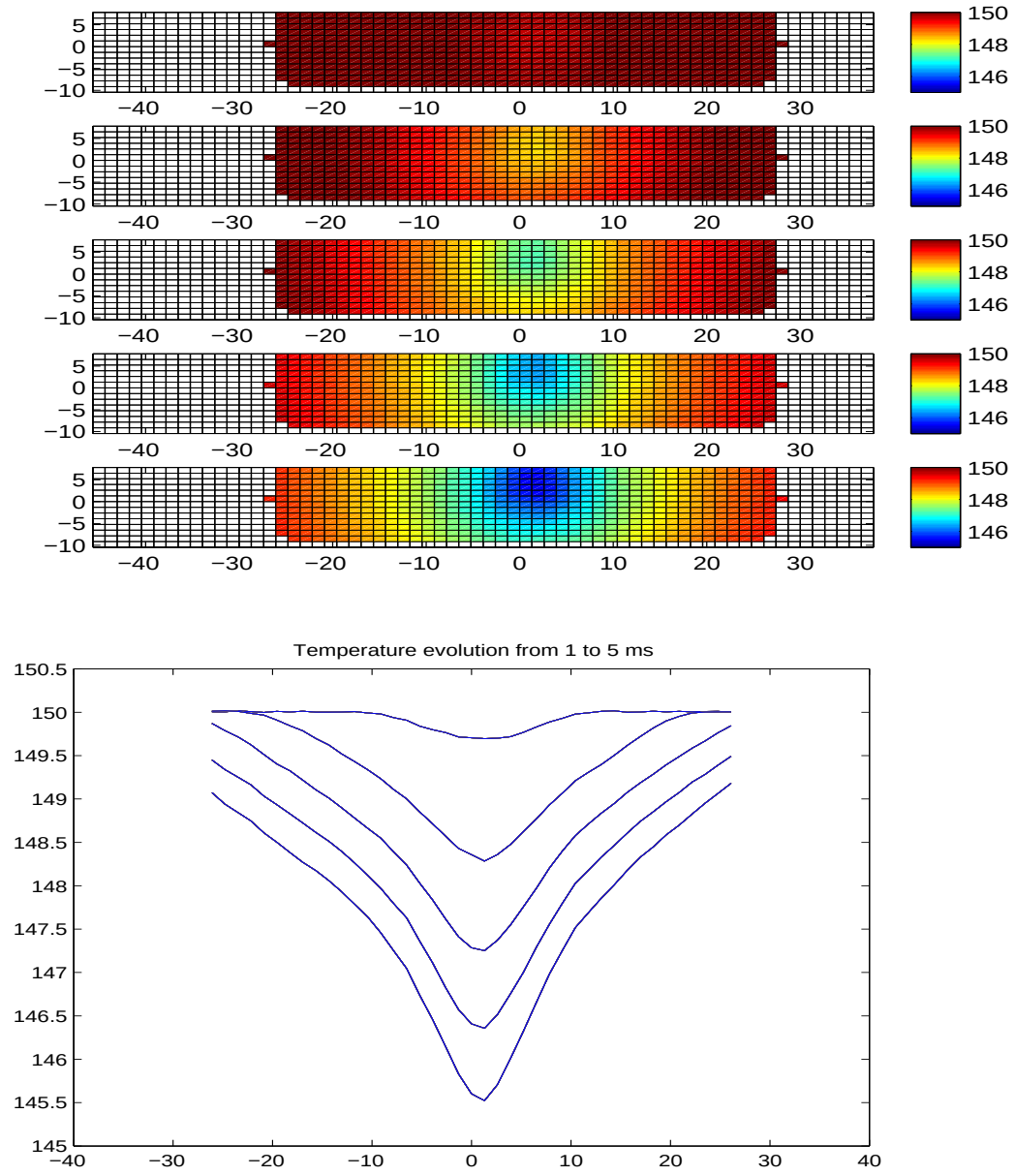

Figure 4.6: zero degrees zoom out case

Thirty degrees case

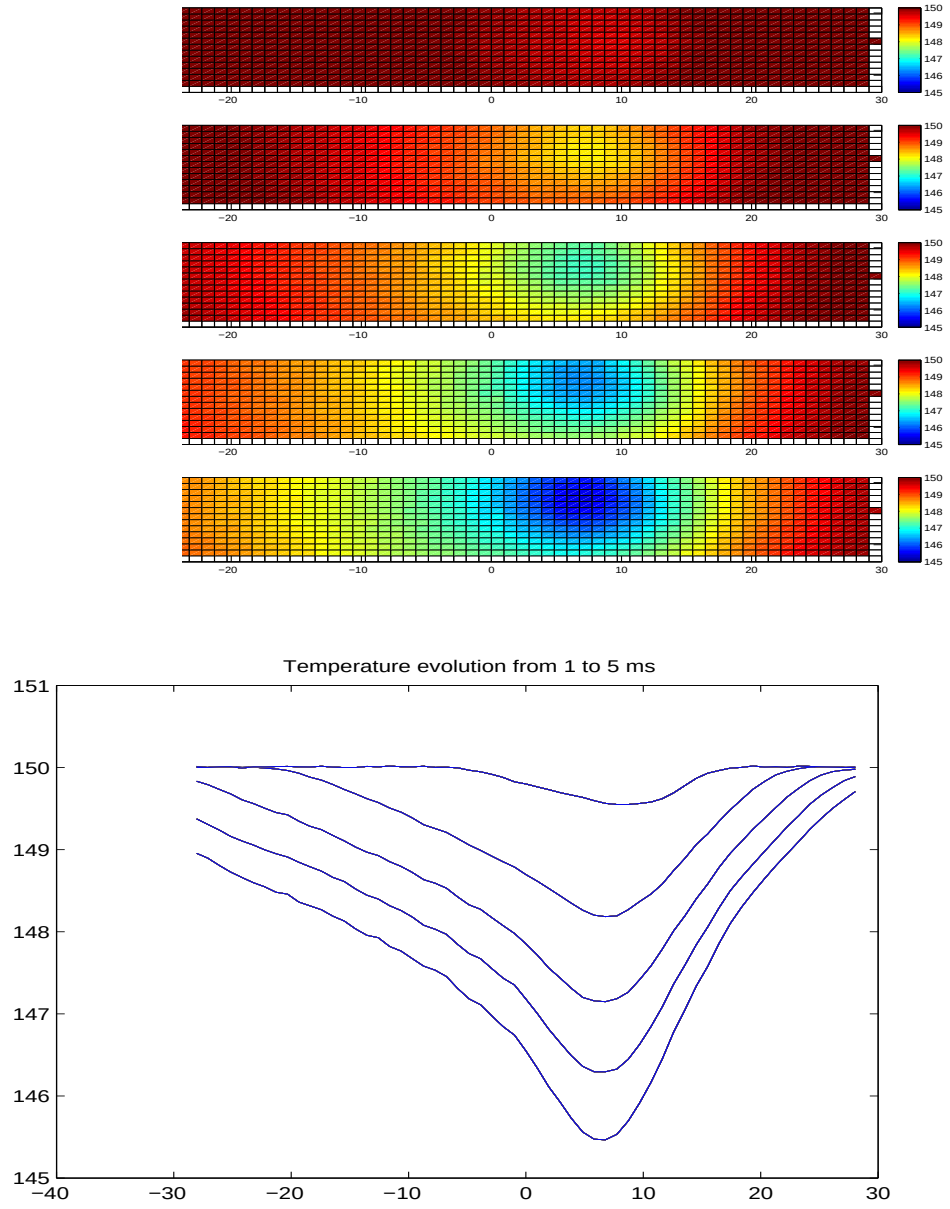

Figure 4.7: Thirty degrees case

Fourtyfive degrees case

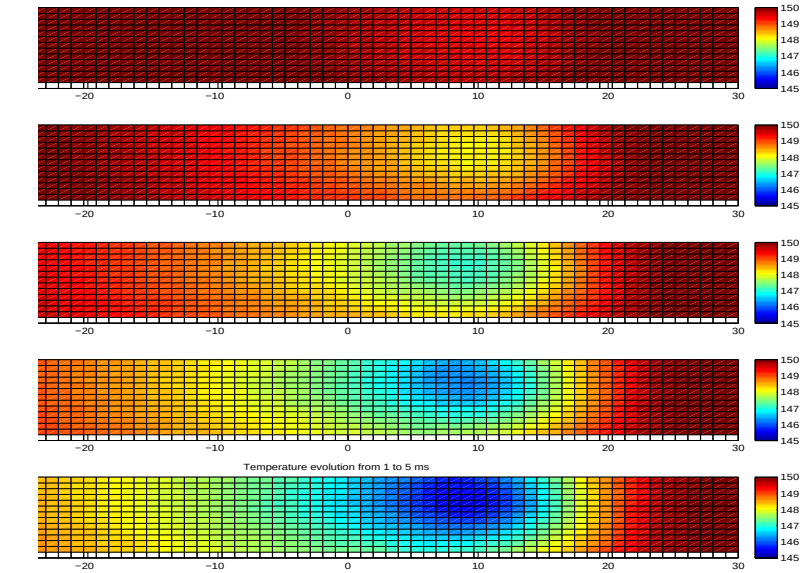

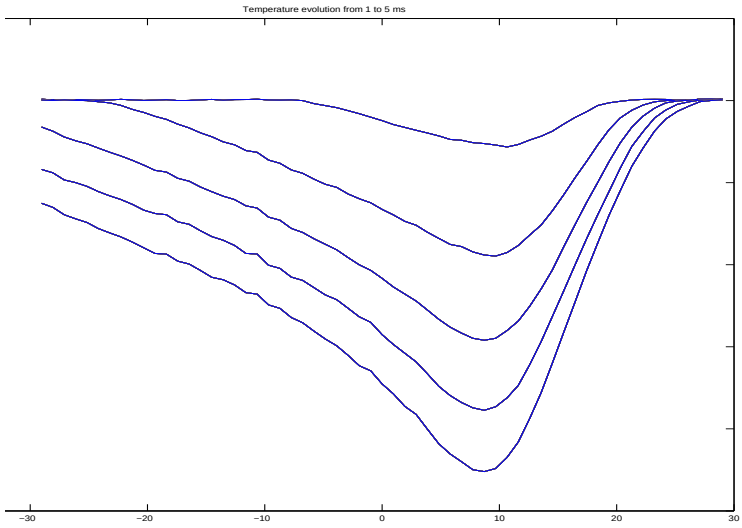

Figure 4.8: Fourtyfive degrees case

Sixty degrees case

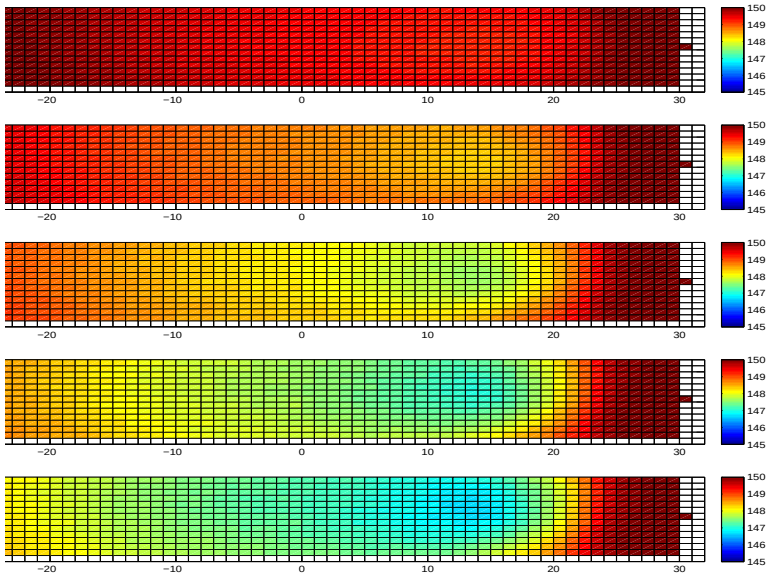

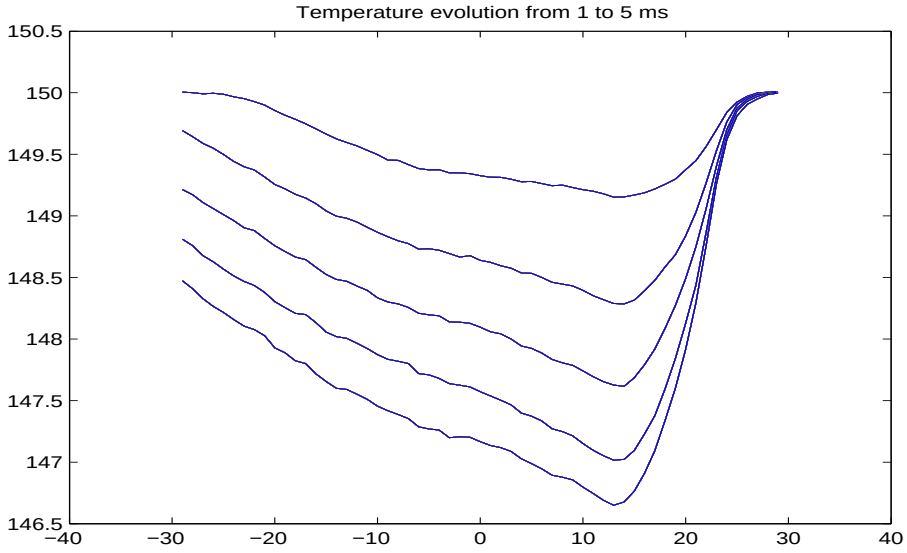

Figure 4.9: Sixty degrees case

Curves comparison

After plotting results for the flat target, all the cases are compared on the graph below.This comparison curve shows the difference response to the jet cooling effects depending on the angle variation. As it can be seen, when the angle between the target and the jet increases, the stagnation point moves up and the temperature change is smaller. Therefore, in the case of 0 degrees is where the biggest drop in temperatures is produced on the jet impact area presenting a symmetric distribution. By contrast, in cases with a significant inclination, we see that the jet fails to reach the part of target located higher up and the jet moves down primarily, resulting in an asymmetric distribution. The maximum recorded temperature gradient is 4.5 degrees Celsius.

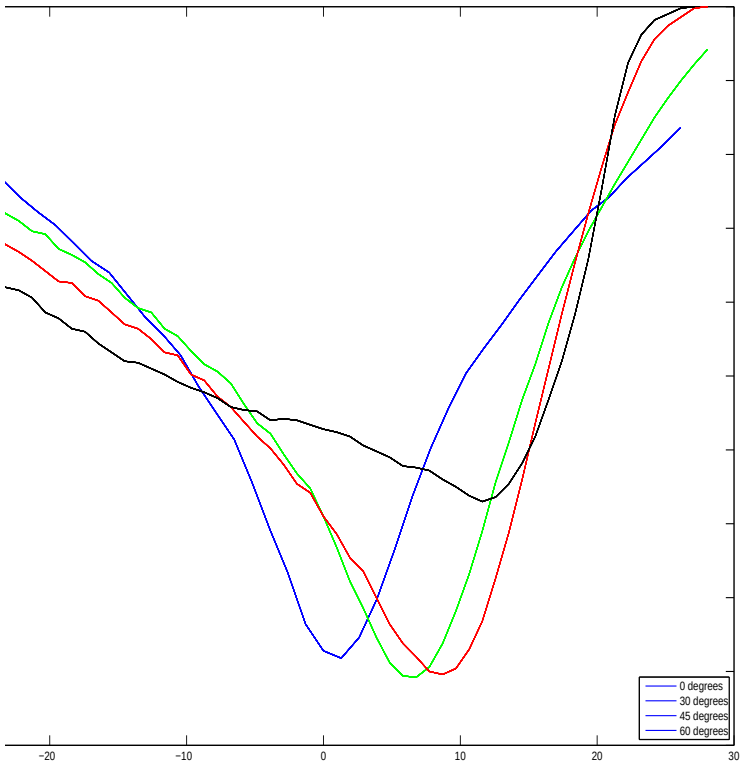

Figure 4.10: Cases comparision

Complete edge case

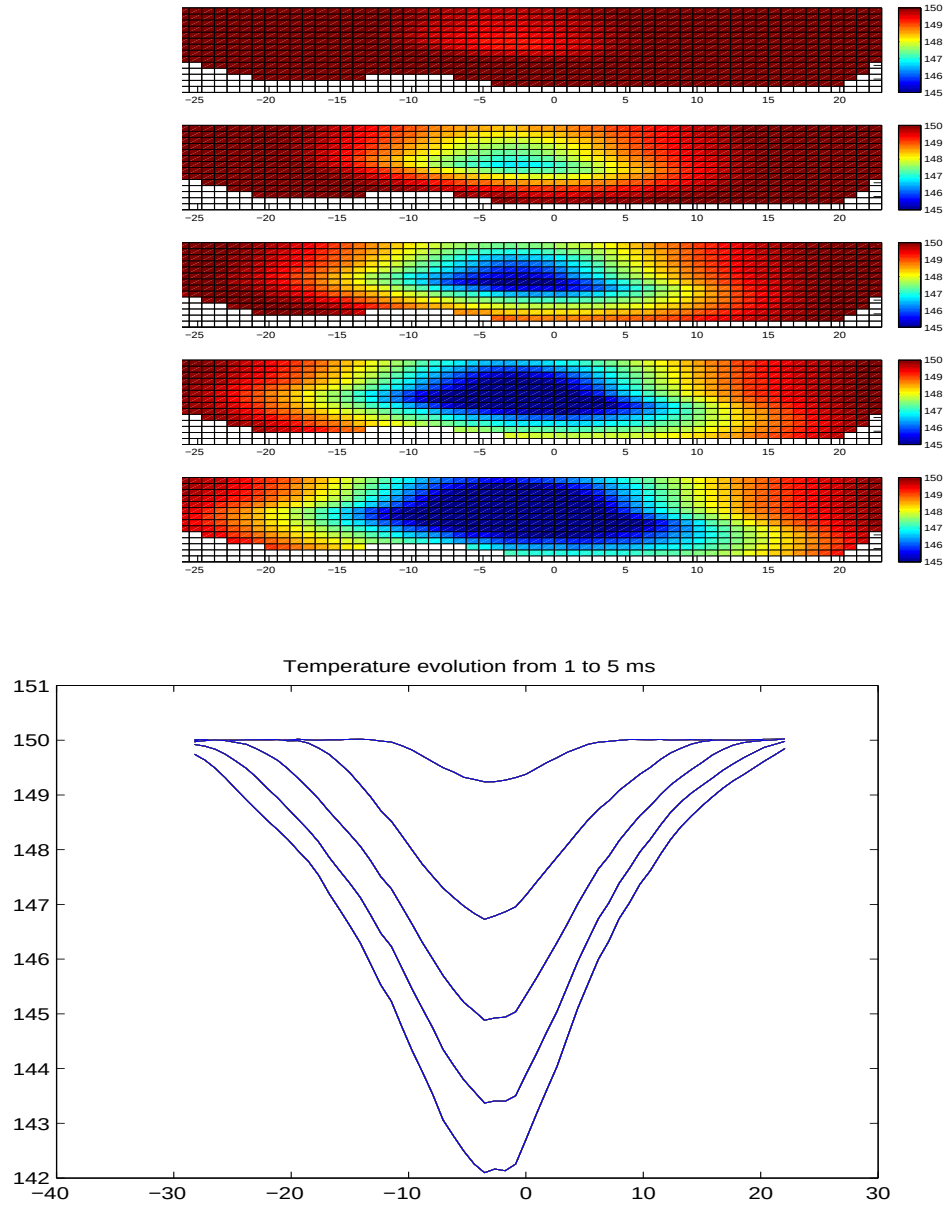

Figure 4.11: Complete edge case

Complete face case

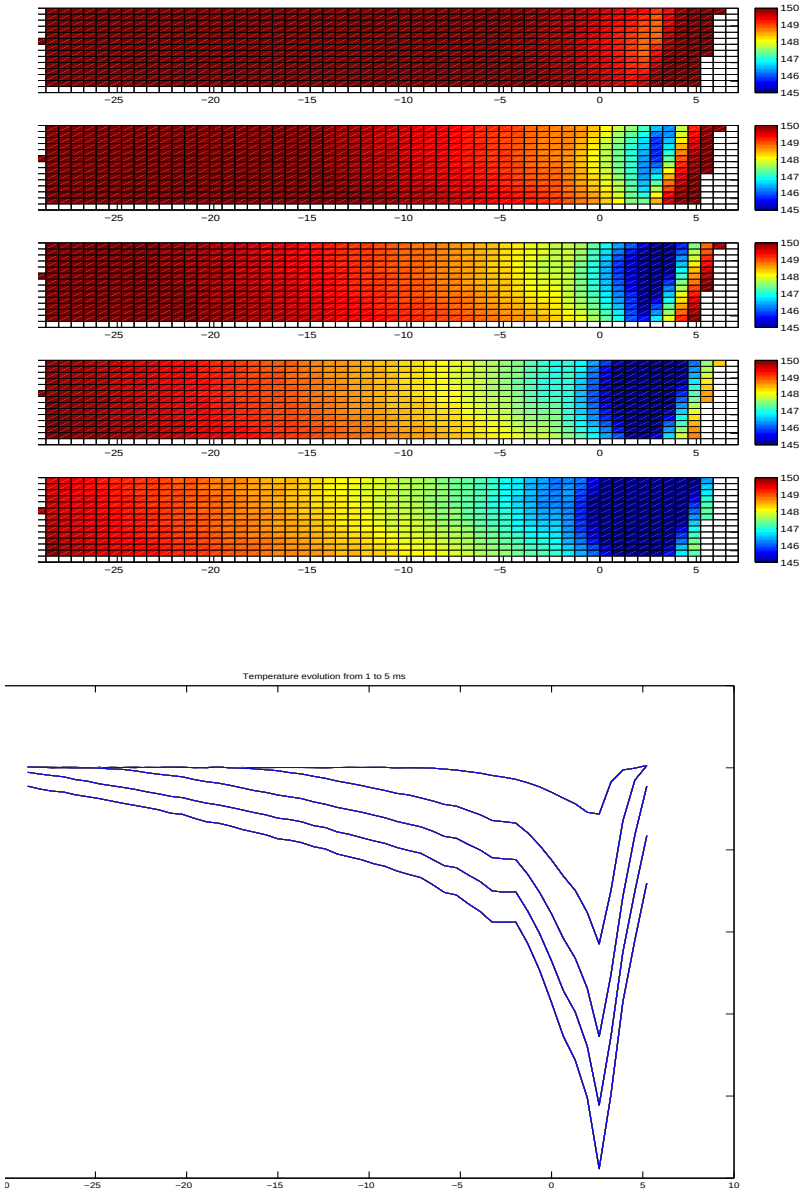

Figure 4.12: Complete face case

Looking to the ninety target case, the thermal effect is bigger than in the flat cases. It can be produced due to the sharp shape of the target that helps

the jet propagation through the surface. Such temperature drop is about 8 degrees and also presents a symmetric distribution reminding to the 0 degrees case. It has to be mentioned that for one of the ninety cases, the complete face case, the data obtained is not really reliable due to the low amount of pixels that represents the jet impact point.

4.2 Conclusions

Comparing the data from the thermocouple analysis and CFD simulations carried out previously [mirko] with the infrared method, the maximum temperature drop is for each is 0.8, 0.2 and 4.5 degrees respectively. For the thermal camera results such a big difference is probably caused by the paint layer. This layer is thick enough to act as isolation in this case; hence the temperature cannot be compared directly to the other methods. However the space distribution and the time evolution can be compared with the thermocouples and the simulation results, and they present a similar behavior. To conclude, the ninety target shows a stronger thermal effect on the edge part compared to the flat cases but a similar temperature distribution. This could explain why the cylinders of modern engines usually break on this area.

Part II

Heat transfer study in Linear Cascade

Chapter 5

Introduction

Demands from industry on improving the efficiency in all kind of energy systems, including aeroengines, are leading to focus on the research of more efficient propulsion systems. There are several ways to increase the energy efficiency in jet engines, i.e. increasing by-pass ratio, raising the combustion temperature, decreasing the weight of the aircraft. This chapter is focused in the study of flow through a fuide vane situated insided a low-speed linear cascade. The heat transfer study performed can help to understand better the complex heat transfer involved in this case. Knowing the heat transfer mechanisms can lead to predict accurateky the maximum temperature that will be achieved in this component and therefore, estimate the cooling (if it is needed) and material suitable for this component.

5.1 Main objective

In this part of the thesis the main goal is to measure the convection heat transfer coefficient on a vane surface and its surroundings (the vane and wall's interaction). The experiment is carried out in a linear cascade and the information obtained can provide a better understanding and knowledge about the heat transfer behaviour of the vane inside a turbine facility, showing which areas suffer a higher heat exchange with the fluid. It is also useful to know the temperature distribution all along the vane surface. In order to calculate this heat coefficient, the heat flux of the wall is fixed.

5.2 Different measurement methods

There are several ways to measure the convection heat transfer coefficient on a vane surface in adition to the infrared method used in this case. The

most common methods carried out nowadays are the thermocouple mapping, the heating foil system and the thermochromic liquid crystal analysis.

5.2.1 Thermocouple mapping

One method used to measure the temperature distribution on the vane is to attached several thermocouples or thermal resistance on the surface. The thermocouples convert the temperature variation into a voltage difference easily to measure with a hight precision. The same happens for the thermal resistances but changing its resistance instead of voltage. The main advantage of this technique is its accuracy, between 0.01 - 0.1 C. Although there are some drawbacks, like the need to use a lot of thermocouples to cover a small surface area.

5.2.2 Heating foil

In this case the vane's surface is heated up directly through heating foils attached on it covering the whole surface. The heating foil provides a total power per each foil that can be measured by the voltage and current. Then knowing the are the flux can be calculated dividing by the area. Furthermore, measuring the surface temperature and air temperature, heat transfer coefficient is calculated. One of the main disadvantages of this system is to ensure a perfect contact between the foil and the vane, when vanes with a complex and high 3 dimensional geometry are used it can be a real problem. Another problem is to ensure that part of heat provided by the heating foil is not going to the inside core of the vane. Furthermore, due to the foil structure, the data acquired can present undulations, which requires a complex post process.

5.2.3 Thermochromic liquid crystal analysis

This method consists into apply a liquid crystal treatment all along the surface, covering the vane with a thin layer. This kind of material is sensitive to the temperature variations, reflecting specific wavelength for each range of temperature. Heating the vane and measuring the temperature distribution on the liquid crystal the heat flux can be calculated and therefore the heat convection coefficient. In this case is necessary to illuminate the scene with white light and record the data with a digital colour camera. This method provides information about the entire surface but liquid crystal are really sensitive to angle variations and they degrade easily.

5.2.4 IR camera

The last technique in use is the infrared analysis, the one chosen. Although it is governed by a different physical principle, the methodology is similar to the liquid crystal technique. But instead of using this material, which is really sensitive to the angle variations, what is done is to cover the vane with an isolating material like rubber or silicone. Then a coating treatment is applied to avoid the angle dependences and reduce as much as possible the radiation reflections from the vane. As in the previous technique with this thermographic method the area covered is bigger and the precision higher, up to 0.01 C. The vane is heated through electrical heaters, an isulating material creates an appreciable temperature gradient which is measured with the IR camera. One of the main advantages is the level of accuracy of this method. On the other hand the main problem from this system is the optical access to vane due to the infrared wavelengths properties, there are really few and expensive materials that are transparent to this wavelength. In this case, due to the dimensions and geometry, little windows are used instead of specific materials.

Chapter 6

Theoretical background

As in any experiment there is always a theory behind it. The theory that supports this experiment and the simplifications and assumptions taken are explained in this chapter.

6.1 Heat transfer mechanisms

In this heat transfer study the three heat transfer mechanisms; conduction, convection and radiation are involved. Therefore each one of this mechanism is explained below. It is also important to mention that in this case the study is done on the steady state conditions, while tge previous experiement was in transient conditions.

6.1.1 Conduction

The heat conduction is generated by the atomic and molecular activity . It is considered as the energy exchange in between those particles with higher energy to those ones with less, trying to reach the energy equilibrium level. This mechanism appears in solids due to the strong interaction between the particles. As soon as there is a temperature gradient inside the solid. The general Fourier law to calculate the heat flux due to conduction is presented as:

$$q'' = -k\nabla(T) = -k(i\frac{\partial T}{\partial x} + j\frac{\partial T}{\partial y} + k\frac{\partial T}{\partial x}) \tag{6.1}$$

where k is the thermal conductivity of the material, ∇ is the gradient three-dimensional operator and T(x,y,z) the temperature field.

6.1.2 Convection

Convective heat transfer is composed by two mechanisms, the energy transfer due to the aleatory molecular movement of the particles (diffusion) and the global or macroscopic fluids movement. This mechanism is characteristic from liquid and gases interacting with another fluid, gas or solid but not between solids

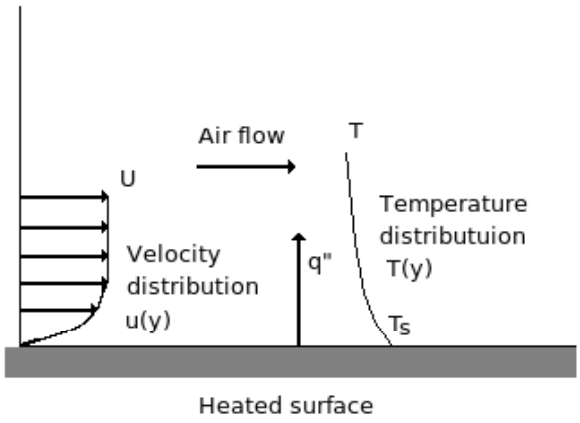

Figure 6.1: Convection between liquid and solid scheme

The equation used to calculate the heat transfer through the convection comes from the Newtons law:

$$q'' = h(Ts - T_\infty) \tag{6.2}$$

where h (W/m^2K) is the heat convection coefficient, Ts the temperature of the surface and T_∞ the fluid temperature, far from the solid surface. In this study, the experimental data obtained with the infrared camera is the T_s from the vane and from the wall in order to be able to measured the h coefficient.

6.1.3 Radiation

The last heat transfer mechanism involved in this case is the thermal radiation. This phenomenon consists on the emission of electromagnetic waves from matter with a temperature above 0 kelvins. Therefore all the bodies emit thermal radiation. The thermal radiation intensity depends on the body temperature and on the wave length considered. Higher temperatures higher radiation heat flux. For each temperature there is a specific wavelength range that implies maximum radiation intensity. According to Plank's law the thermal radiation intensity, as a function of temperature and wavelength for black bodies is described as:

$$I_\lambda, b(\lambda, T) = \frac{2hc_0^2 m}{\lambda^5(e^{\frac{hc_0}{\lambda KT}} - 1)} \tag{6.3}$$

where $h = 6.6256x10^{-34}$ Js and $1.3805x10^{-23}$J/K are the *Planck's* and *Boltzmann* universals constants respectively, $c_0 = 2998x10^8$ m/s the light speed, T the absolute black body temperature in Kelvins and λ the wavelength. Black bodies as a diffuse emitter, have a uniform spherical radiation, then the spectral emissivity power is known as:

$$E_{\lambda,b}(\lambda, T) = \pi I_{\lambda,b}(\lambda, T) = \frac{C_1}{\lambda^5(e^{\frac{C_2}{\lambda T}} - 1)} \tag{6.4}$$

where $C_1 = 2\pi hc_0^2 = 3.742x10^8 W\mu m^4$ and $C_2 = hc_0/k = 1.439x10^4 \mu mK$ This distribution, represented on the next figure, shows the energy emissivity depending on the temperature and the wavelength for a black body.

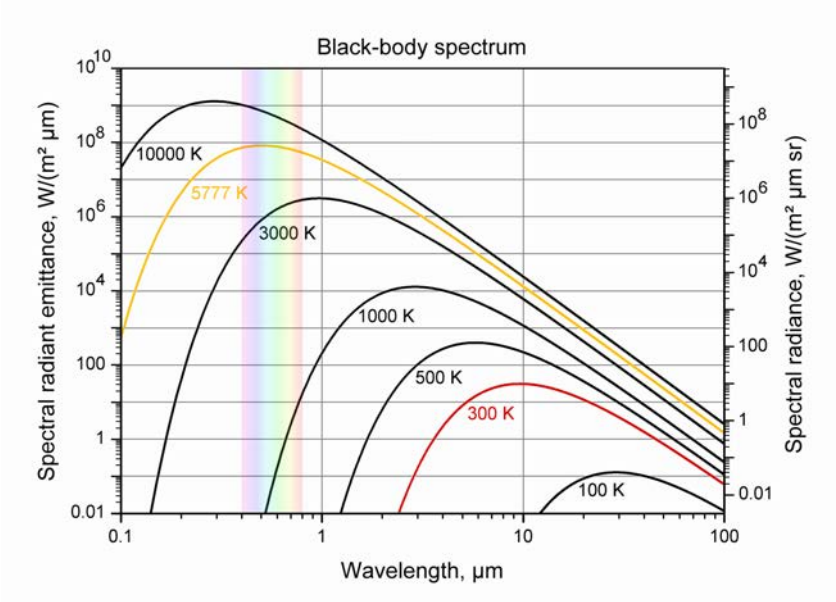

Figure 6.2: Blackbody spectrum

As can be seen, the radiation varies continuously with the wavelength and the radiation emissivity increase while increasing the temperature for each wavelength. Also in the main cases the smaller wavelengths provide a higher radiation emissivity, showing a linear relation between the λ maximum and the body temperature.

Applying the *Wien displacement* to this distribution $\lambda_{max} = 2897.8 \mu m K$ the emissivity power can be expressed only as a function of the body temperature:

$$E_b(T) = \int_0^{\infty} \int_0^{2\pi} \int_0^{\pi/2} = I_\lambda, b(\lambda, \theta, \phi, T) \cos\theta \sin\theta d\theta d\phi d\lambda \int_0^{\infty} E_\lambda(\lambda) d\lambda \tag{6.5}$$

Simplifying for constant wavelength the equation above turns into:

$$E_b(T) = \varepsilon \sigma T^4 \tag{6.6}$$

where ε is the emissivity factor of the body (1 if it is a black body, 0.973 in our case because is the emissivity of the coating treatment) and $\sigma = 5.66910^{-}8 W/m^2 K^{-}4$, the *Boltzmanns* constant.

6.2 Model analysis

Once is known what is the theory behind the experiment it is time to apply it for the studied case. The three main heat transfers mechanisms

mention before are involved; conduction, convection and radiation. Using the formulas described on the previous section, an energy balance is applied above the surfaces of the vane and of the wall. Hence, applying the energy conservation and knowing that the heat flux that goes into a volume of control has to be the same that goes out:

$$q_c'' = q_h'' + q_r'' \tag{6.7}$$

The conduction heat, that cross the silicone rubber layer of the vane and the plexi of the wall, has to be the same as the convection and radiation heat between the surfaces studied with the camera and the surroundings. Figure 6.3 ilustrates this heat balance.

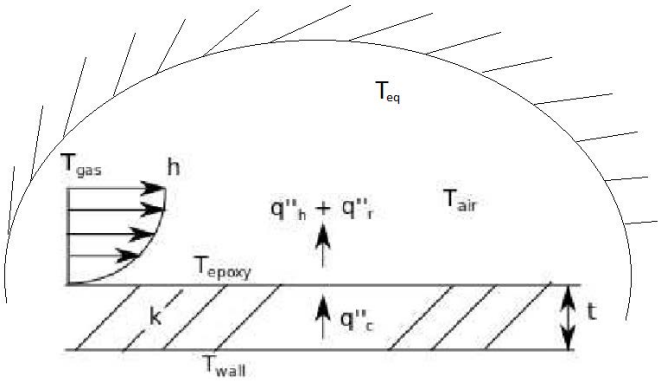

Figure 6.3: Heat balance

Applying the heat transfer formulas:

$$q_c'' = -k\nabla T = \frac{k}{e}(T_{al} - T_{surf}) \quad \text{Conduction heat flux} \tag{6.8}$$

$$q_h'' = h\Delta T = h(T_{surf} - T_{air}) \quad \text{Convection heat flux} \tag{6.9}$$

$$q_r'' \approx \sigma(\varepsilon_{surf} T_{surf}^4 - T_{eq}^4) \quad \text{Radiation heat flux} \tag{6.10}$$

where k represents the thermal conductivity coefficient of the silicone rubber from the vane and of the plexi from the wall, e is the thikness of the covering layer, which is 3 mm and 5 mm for the vane and wall respectively. T_{surf} is the surface temperature that is measured with the infrared camera,

the vane surface and the wall surface. T_{al} is the temperature of the aluminium plate and the vane's core for each case. In equation 6.13 h is the heat transfer convection coefficient, T_{surf} the temperature of the vane and wall surface, T_{air} is the temperature far enough of the boundary layer and T_{air} is the ambient equivalent temperature. In addition σ is the *Boltzmann* cosntat and ε_{surf} the emissivity of the measured surface.

Substituing on the heat balance:

$$\frac{k}{e}(T_{al} - T_{surf}) = h\Delta T = h(T_{surf} - T_{air}) + \sigma(\varepsilon_{surf}T_{surf}^4 - T_{eq}^4) \tag{6.11}$$

then h is calculated as:

$$h = \frac{\frac{k}{e}(T_{al} - T_{surf}) - \sigma(\varepsilon_{surf}T_{surf}^4 - T_{eq}^4)}{T_{surf} - T_{air}} \tag{6.12}$$

Chapter 7

Experimental components

This experiment consists in the temperature measurement of an instrumented vane and a linear cascade wall with an infrared camera. In this chapter the vane and the wall characteristics, such as their design, geometry and manufactured are explained in more detail

7.1 The wall

The main objective of the wall is to find out which is the heat transfer coefficient on the vanes surroundings, particularly on the vane and interaction. In order to be able to measure such coefficient what is done is to set two uniform temperatures on the wall (heating it) to know exactly the conduction heat flux coming from the window. One of these known temperatures is placed inside the wall, in contact with the warm part, and the other one on the surface (the one that is measured with the camera). A plexi layer separates them creating a sensitive temperature gradient.

7.1.1 Design and wall simulation

Before building the wall a brief simulation is done to check different design, geometries and configurations and to ensure that the window will present an uniform temperature al along its surface, in both layers.It is crucial to have an accurate estimation about how will the walls behaviour be in reality and which parts are critical (the ones with a non uniform temperature distribution) and to guarantee that the heat flux goes where is supposed. The wall simulation presented isotherms on the x axis, so we can assume that the temperature on the plexi and the aluminium are uniform, anyway this will be checked during the experiment setups. It is also important to notice that

practically all the heat flux goes to plexi as planned.

7.1.2 Wall components and geometry

After running the simulation the definitive wall dimensions and wall components are set. The wall is composed by two aluminium plates, one plexi layer, four rectangular heaters and an isolating plastic frame which holds all the components.

-Dimensions:

- Front aluminium thick plate: 364 x 938 mm, 10 mm of thickness.
- Back aluminium thin plate: 322 x 896 mm, 5 mm of thickness.
- Plexi plate: 414 x 988 mm, 5 mm of thickness.
- Heaters: 190 x 330 mm, 3 mm of thickness
- Frame: 440 x 1014 mm. See figure 7.1 for details.

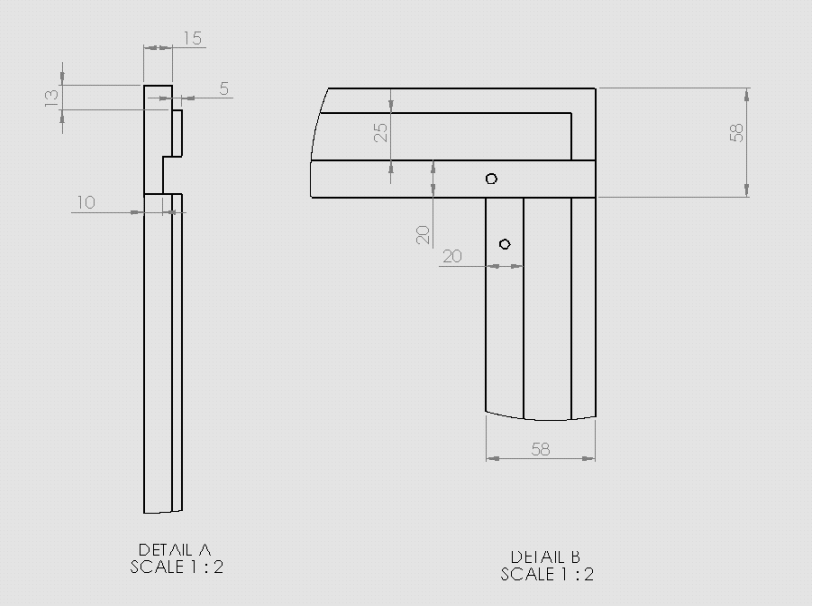

Figure 7.1: Frame detailed views

Figure 7.2 shows the exploded view of the wall components, not including the heaters.

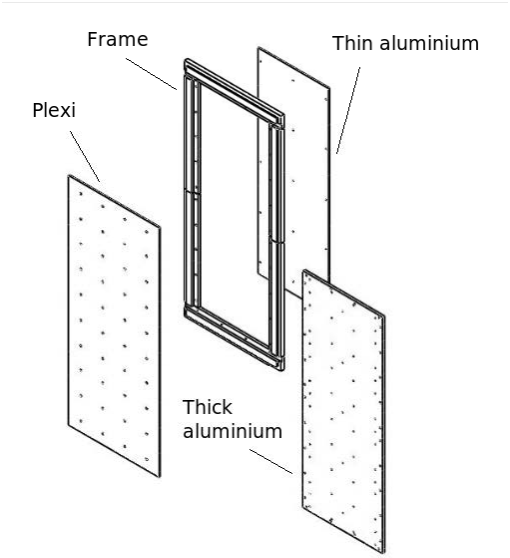

Figure 7.2: Exploded view of the wall components

7.1.3 Wall assembly

The assembly procedure is the following. First the thick aluminium plate is attached to the frame through metallic screws, then the heaters are placed on the back of this aluminium plate. Thermal paste is used to ensure that there is no air gap between the heaters in order to avoid that this gap could act as isolation between them and ruin the experiment. Obviously, the thermal paste has a significantly lower thermal conductivity than the aluminium but it is still much better than the air (0,02 W/m^2K. Next step is to put the thin aluminium plate over the heaters to press them into the thick wall and provide a better contact, the thermal paste is also applied on the thin aluminium to improve the sealing conditions. Metal screws are used as well. The last step is to screw the plexi glass to the front part of the wall, in this case it is really important to mention that the screws used are made of plastic. The main reason is to avoid heat flux leakage through the screws, it would happen if they were made of steel or any other metal like aluminium. After all the wall is ready for the testing process explained later on the experiment setup chapter

7.2 The instrumented OGV

7.2.1 Vane characteristics

The vane is the main target under study. Its geometry is given by GKN company and manufactured by a workshop. It is made of aluminium, which is really suitable for this heat transfer study due to its high heat conduction coefficient (about 210 W/(mK)). It has three cylindrical passing holes through the section to place the heaters.

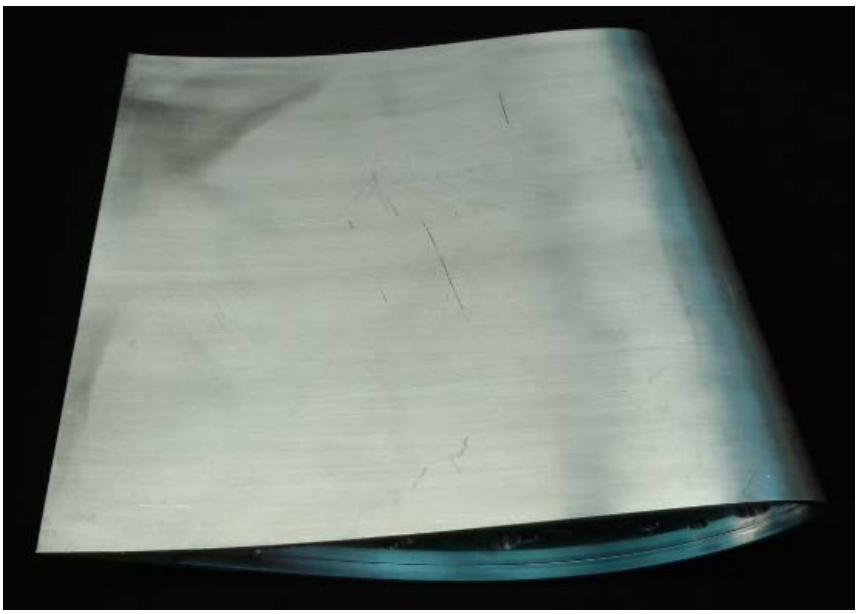

Figure 7.3: Vane under study

As is mentioned in the introduction part there are several techniques, such as heating foils, liquid crystals, etc. to measure the heat flux on a vane and consequently the heat transfer coefficient. On previous cases these methods were not satisfactory at all so in this case a different technique used recently which showed good results is applied.

Following the same principle as in the wall, one layer of low conductivity material is needed to produce an important temperature gradient between the heated aluminium vane and the measured surface to determine the heat conduction flux. In this case a 3 mm silicone rubber is glued covering the entire vane surface, this carefully glueing process is done with Borjas Rojo collaboration. The main problem that comes up from this process is the possible emergence of air bubbles during the glue application and drying process. This fact is really important for the heat transfer study because

these bubbles can create cooler areas on the silicone surface due to the airs low conductivity. If the bubbles are significantly big they can affect to the measurements and ruin the experiment.

7.2.2 Silicon gluing process

In this section the steps followed to cover successfully the vane with the silicone are described . First of all the vane needs to be fix and supported on a structure, in this case a metallic one made it with beams. Then a piece of silicone rubber is cut a bit longer than the entire vanes surface dimension. It is very important to clean both, the silicone rubber and the vane with alcohol before the gluing to avoid anything that could disturb the sticking or produce some irregularities on the surface. After this we proceed with the glue, in this case the one used is a conventional liquid glue which can be found in any hardware store. The main advantages of this kind of glue is the low speed of solidification, which is useful in order to have enough time to work until it dries and the grade of viscosity, which makes it easy to spread the glue over the vane. Before applying the glue, one extreme of the silicone piece is attached and tightened to the metallic structure to fix its position. Then an horizontal row of glue is applied from side to side on the vane surface. We press the glue with the silicone, to spread it, using a metallic cylinder to in order to apply an uniform and stronger force. This action is repeated all over the vane until the silicone covers the whole aluminium core. Then the other extreme of the rubber piece is also fix to the metallic structure, to apply tension. It has to be mentioned that in this gluing process some problems appeared and this action was repeated several times to reach the enough grade of precision. However very little bubbles appeared on the leading and trading edge, but they are small enough to not affect the results and far from the area that is measured.

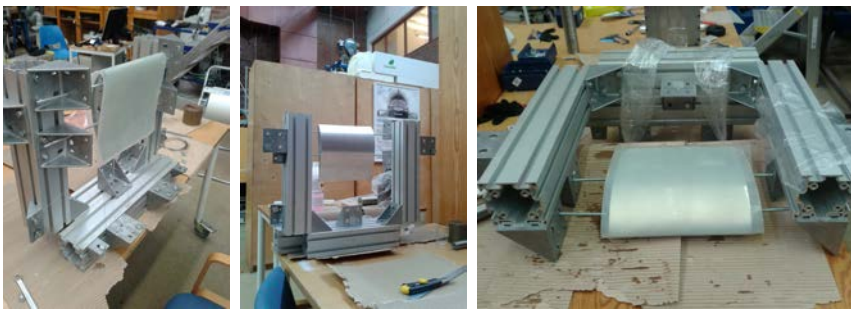

Figure 7.4: Gluing process

Chapter 8

Linear Cascade

The heat transfer experiment is run in the Chalmers subsonic Linear Cascade. This rig was built in 2004, it has been a useful tool to understand much better the flow fields around the outlet guides vanes in jet engines. In our case is used to have a deeper knowledge about the vane's heat transfer. It is also a great device to validate computed fluid dynamic models (CFD). The main purpose of the linear cascade is to obtain experimental data that could help to improve the efficiency in gas turbines in order to reduce fuel consumption and gases emissions.

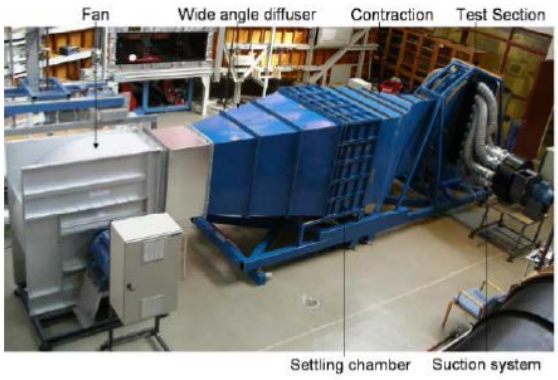

Figure 8.1: Test facility

The testing area of the linear cascade, where the vanes are placed has a cross section dimension of $1200x200mm^2$. The inlet wind speed are variable up to a maximum of 20 m/s. In this testing area it is possible to install different kind of vanes and mount many configurations, that's possible thanks to the replaceable walls. These walls are made of transparent glass what makes easier the optical measurements. In our case one of this walls is the instrumented and measured one, on the other hand the opposite wall needs to be customized due to its opacity for infrared wavelengths. Another important advantage is the possibility of running experiments under realistic *Reynolds* numbers.

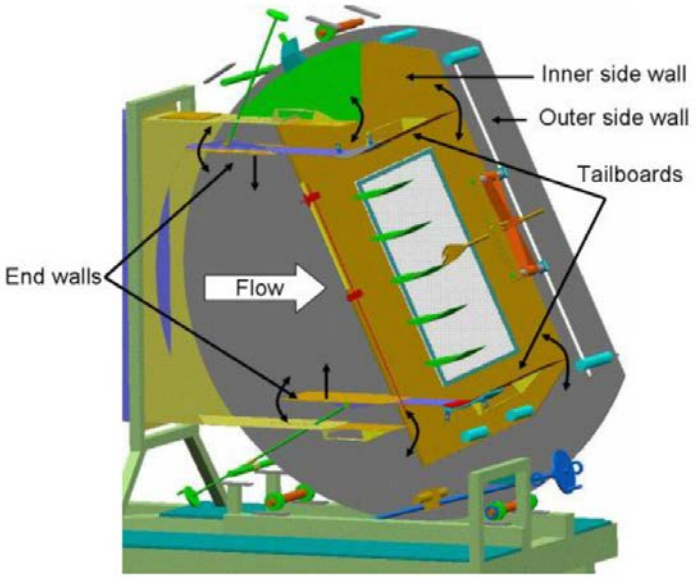

Figure 8.2: Testing area

The angle between the studied vanes and the inlet air flow can be modified in a significant range, from 0 to 52 degrees, this fact combined with the previous one increases highly the variety of design and drift conditions than can be studied.

The linear cascade also permits to introduce grids upstream the test section, what means that it is possible to introduce turbulence, allowing to have different levels of turbulence in the approaching air stream. Two traverse systems are placed upstream and downstream the studied vanes, very useful when wide flow field mappings are required. There is also an advanced suction system that can control on the testing area walls the growth of the boundary layers.

For this experiment the linear cascade configuration is set to 20 m/s and the vanes to the *on design* configuration, it has to be remarked that the instrumented vane is placed on the second position from the top.

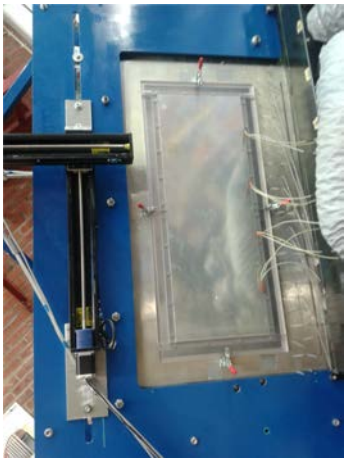

Figure 8.3: Studied wall installed on the linear cascade testing area

Chapter 9

Measurements set ups

Before running the experiment there are some things that must be set up and checked. The infra red thermal camera is configured and calibrated for the data collection, the uniform temperature distribution of the wall is checked, a painting treatment is applied above the two studied surfaces and the optical acces for the camera is design and manufactured.

9.1 Camera setups

The infrared camera used for this experiment is the same as in the previous one, a MWIR Phoenix Camera System with a 320x256 resolution. The main difference between the other experiment is the type of lens used. For the transient heat transfer experiment the lens of the camera was narrower due to the little area covered. In this case a wide vision field is needed so that the camera objective is changed for a new one. This lens offers an entire view of one vane path at a relatively short distance.

9.1.1 Basic configurations

Some basic camera configurations are setted first. The main value to fix is the integration time of the camera. In this case the range of temperatures under study are from 25 to 55 degrees. What is done is to find a suitable integration time for this range of temperatures, having a number of counts close to the maximum admitted for the camera (16000). In our case the integration time is fixed at 1.2 ms looking at a 50 uniform temperature. This uniform temperature is provided by a calibration device used also in the *Part I* , but with some modifications. This device had a metallic conical structure around the plate before, this structure was removed and the plate was turned

upside down and holding between two beams to avoid the possible convection effects that could disturb the calibration measurements. The picture below shows this calibration device and the camera position.

Figure 9.1: Studied wall installed on the linear cascade testing area

Another basic configuration is the window size of the camera, in this case it is the maximum that the camera can offer, because the optical area covered needs to be as biggest as possible. This window size is 320x256 pixels, at this size the frame speed of the camera is the lowest one (122 frame per second) but considering a steady case study this fact does not affect us.

9.1.2 NUC and calibration

The non-uniformity correction of the camera detectors is needed to be done as well, like in the first experiment. In this case the cold and hot temperatures used are 25 ^oC and 55 ^oC respectively. Regarding to the camera calibration curve, the 5 temperatures selected are 25, 32.5, 40, 47.5 and 55 ^oC because that is the temperature working range for the experiment.

9.2 Wall checking

One of the most important parts for the experiment success and validation is to confirm that the end wall designed gathers the expected conditions. The heated wall has to show an uniform temperature distribution all over the plexi surface.

First of all what is checked is if the opposite aluminium layers presented the same temperature in both sides of the heaters (due to the high aluminium

conduction coefficient). The wall is mounted but without the plexi layer and several thermoresistance are placed in both aluminium plates. Then the heaters are connected to a transformer that supplies electrical current. The temperature of the thermoresistances is monitored through the time until the steady state. The result of this comprovation is a maximum difference of 0.1 degrees between opposite points, which belongs to the measurement error of the thermal resistances, and between different position points on the plate was 0.2 degrees. After this checking we assumed that both aluminium layers present the same temperature distribution, acting as a mirror.

After this three thermal resistances are attached on the aluminium thin plate to know its temperature during the experiment.Then the back part of the wall (where the thin aluminium is placed) is covered by isolating material to force the heat flux to go to the front part, to the thick aluminium layer and the plexi. Three holes are made to let pass the thermal resistance and heaters wires (see figure 9.1). Once the isolation is ready the wall is heated to check again the temperature on the 3 back points, as before the maximum difference is about 0.2 - 0.3 degrees. So we still assume that the wall has an uniform thermal behaviour.

Figure 9.2: Wall after back isolation

Finally, the last wall checkout is done with the thermal camera. For this process the plexi part is attached with plastic screws, and the surface treatment (which is explained in the next section) is applied. Then the wall is heated up until the steady state and the plexis surface is acquired with the camera. In this case the maximum temperature difference was sensitively bigger than before, up to 0.7 degrees, but it is important to say that this is due to the natural convection of the wall. Figure 9.2 shows the camera

capture for the heated wall, as it can be seen the coldest parts are obviously the extremes of the wall, specially the corners.

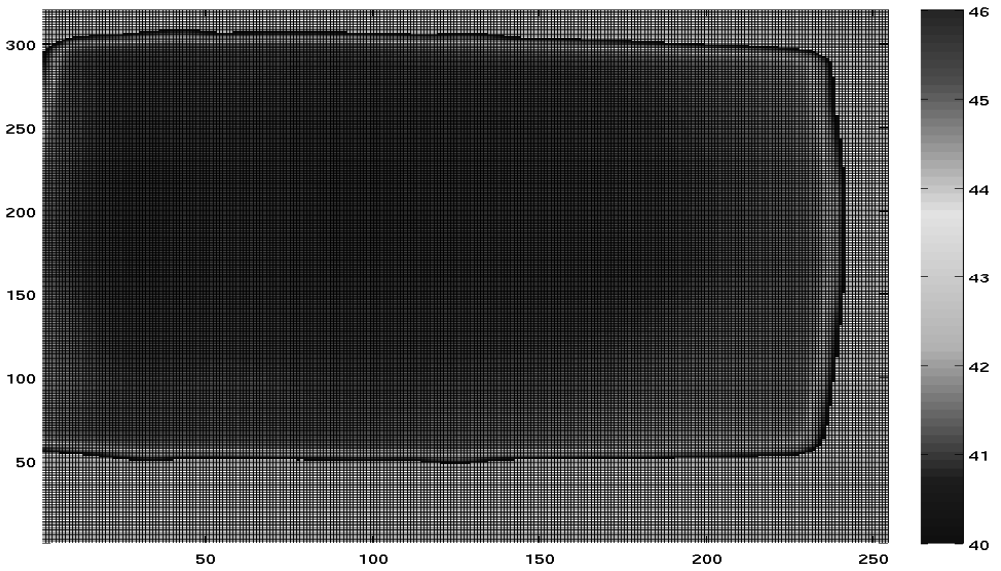

Figure 9.3: Camera capture of the heated wall

9.3 Surface treatment

On the surface of the vane and on the plexi plate, a painting treatment is applied as on the targets from the *Part I* experiment.

9.3.1 Black coating

In order to make the studied surfaces act as a blackbody, they are painted with the a special coating Nextel Vetel-Coating 811-21 from Mankiewicz Gebr. & Co. This paint has an emissivity factor of 0.973 (almost 1 as the blackbodies) which is perfect for the experiment. It also has a very low angle dependence, another important reason that makes it suitable. To paint both surfaces a spray gun is used in order to make the paint layer very thin and smooth to not disturb the measurements.

Figure 9.4: Vane and wall after the coating treatment

9.3.2 Positional marks

Apart from the coating treatment the vane and the wall need to be marked to reference their geometry to a coordinate system. What is done is to mark several points all along the surface with a silver marker, this kind of silver pen has an emissivity factor lower than the coating, which permits to differentiate the points from the rest of the surface while looking through the thermal camera. The coordinates of the points are extracted from the ICEM CAD design. The vane geometry is cut by 3 profiles, in each profile there are several points representing the curve.

For the wall it is much easier because it is a flat and 2 dimensional surface, in this case the points chosen correspond to the geometrical position of the plastic screws. What is done is to mark with a silver dot the centre of some screw. Figures 9.4 represent the vane and the wall after this marking process.

9.4 Optical access for the camera

Once the vane and the wall are ready for the experiment, they are placed into the linear cascade testing area. Now what comes up is how to place the camera in order to be able to capture the area of interest. As it was said on previous sections, the infrared camera can not see through the glass due to its wavelength sensivity. The plexi window acts as an opaque surface. Hence, there is the need of solving this problem. The first option was to make several holes in the window and put sapphire, which is supposed to be transparent for the infrared wavelength, 3 to 5 μm. But this fact was not true at all, several sapphire crystals were tried with the camera but they still reflected some of the infrared light, so to avoid this kind of reflections and also for the expensive price of this type of glass this solution was discarted. In figure 9.5 there is a picture taken using this sapphire glass and it can be seen how the camera objective (the ring shape) is reflected on the sapphire glass.

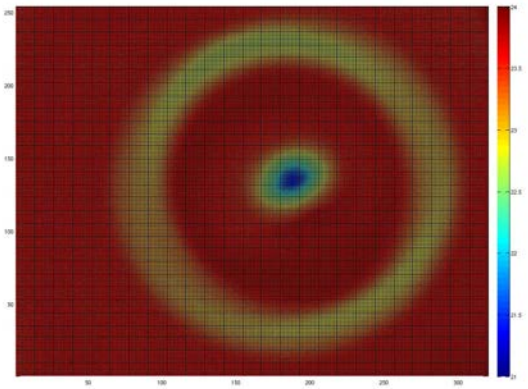

Figure 9.5: Picture taken with sapphire crystal

After refusing the sapphire option, the solution proposed is to drill two little windows on the glass wall. This windows remain closed while the cascade is running. They are just opened no more than 1 second to take the pictures with the infrared camera, avoiding the flow disturbance. In this case the windows are considerably big (125 x 170 mm) because one whole path and both endings parts of the two vanes are photographed. The opening system for these windows consist into fix them with two hinge with springs, so they remain closed thanks to a stopper and as soon as it is removed, the windows are opened automaticaly and the picture is taken. The design of

these windows is made carefully considering the distance required for the windows apperture and the camera postion. Due to the precision required for this windows, owing that there cannot be any gap or irregularity that could alterate the air flow, the manufactured is done by a workshop.

After this, all the preparations for the experiment are done and we are ready to mount all the parts into the linear cascade and to measure and record the data using the infrared camera. Figure 9.6 is a sketch of how does it looks the ensemble.

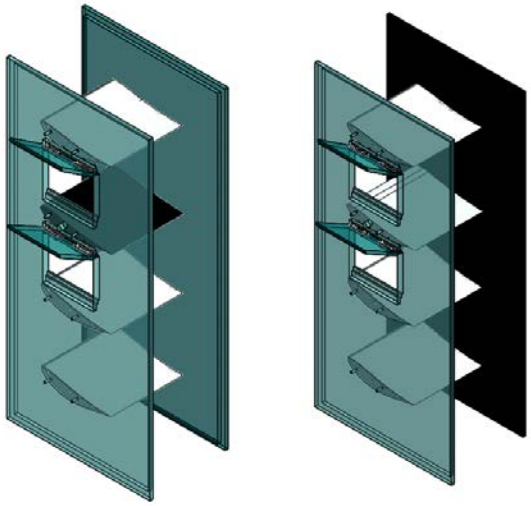

Figure 9.6: Overview of the mounted parts

Chapter 10

Results

10.1 Post process

Once the pictures are made with the IR-camera, the data obtained needs to be transformed into useful information. First of all, what is done is to convert the 320x256 matrix of counts into a temperature matrix in Celsius. To do this, the calibration polynom is applied. In the figure below we can see on of these pictures after transforming the counts into temperature.

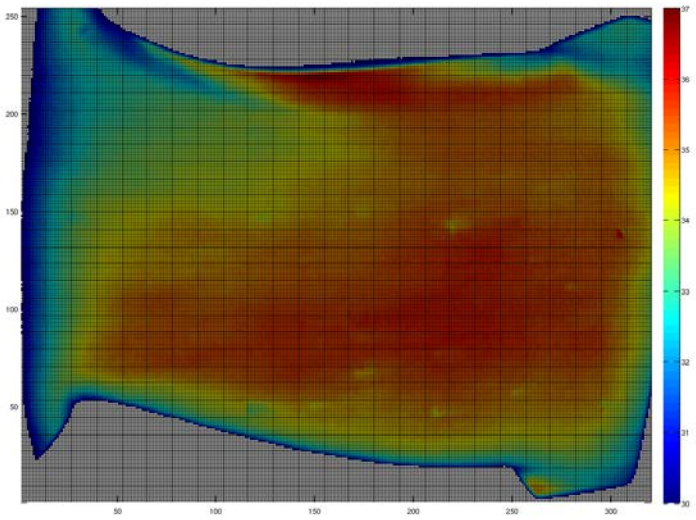

Figure 10.1: Picture after applying the polynom

Next step is to apply a filter to the images in order to erase that informa-

tion that is not useful for us, like the outsides of the wall. Another good point is to fix the temperature map into a more accurate scale. Figure 10.2 shows one of the images after applying this filter. This action can be repeated as many times as necessary until the desirable information is clearly seen.

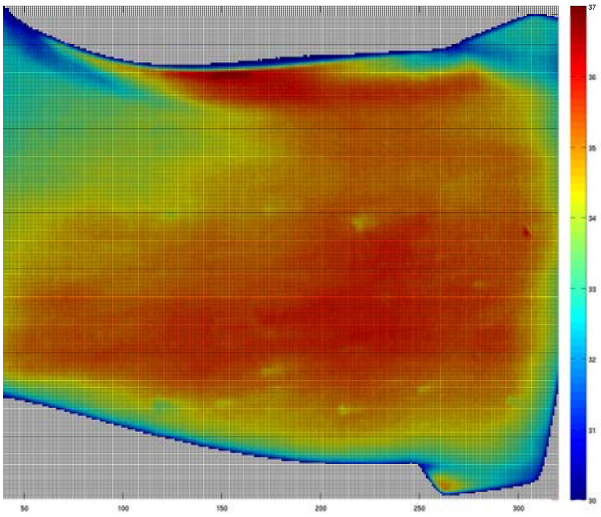

Figure 10.2: Picture after filtering

Then the 2-D picture needs to be transform into the real 2-D geometry. Every silver point represents a known coordinate so we can place all the points of the picture to represent the three dimensional geometry of the the targets. Interpolating all the pixels of the picture using the reference of the marks. Some parts of the vane and of the wall are not possible to acquired due to the geometry and specially to the optical access that the camera has. That is why some parts are not represented.

Finally the silver marks, made during the experiment setups to be able to referenced the geometries, are removed. To remove them what is done is to interpolate the marked area with the information from the surrounding points. This action is made manually selecting the area of the point. The interpolation used is a 2D cubic one. Figure 10.3 shows the picture before and after removing the silver points.

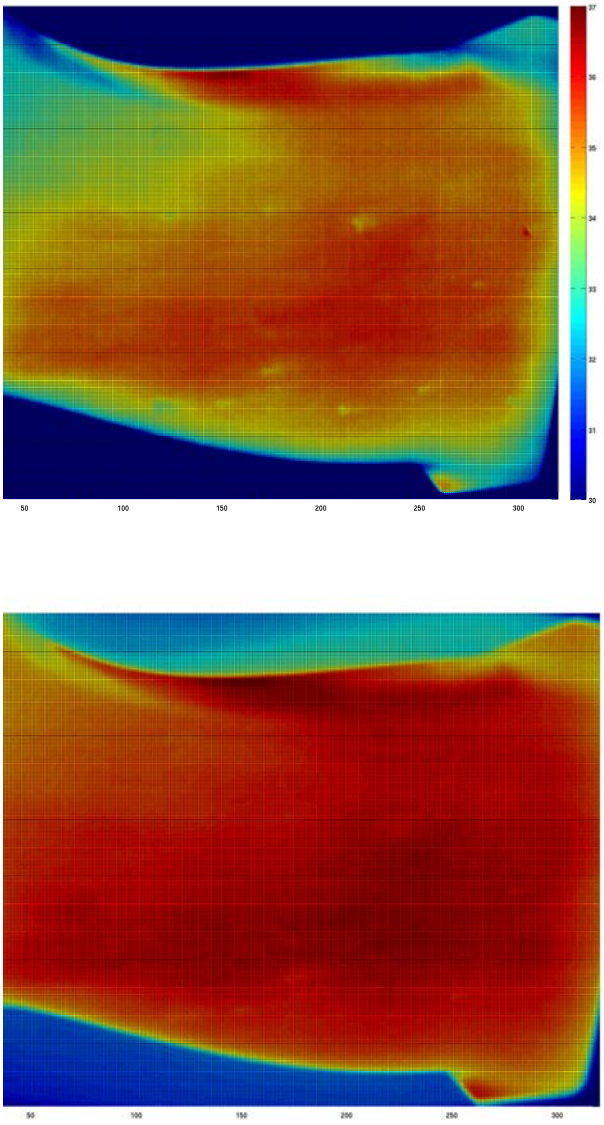

Figure 10.3: Before and after removing the silver marks

10.2 Experimental results

After post-processing the pictures the information obtained is exported to the CFD software FLUENT. Using this software the temperatures measured on the surface with the camera are setted as a boundary condition, more over the vane core temperature is also fixed as boundary condition (what we measured during the experiment) and the aluminium plate from the wall as well. Also the air temperature for the convection and radiation heat transfer calculations is measured and fixed.

So, when all the boundary conditions and the material properties are fixed the h coefficient is calculated over all the studied surfaces applying the theoretical model described previously. The upper and lower path come together, showing on figure 10.4 the distribuiton of the heat transfer coefficient along the end wall.

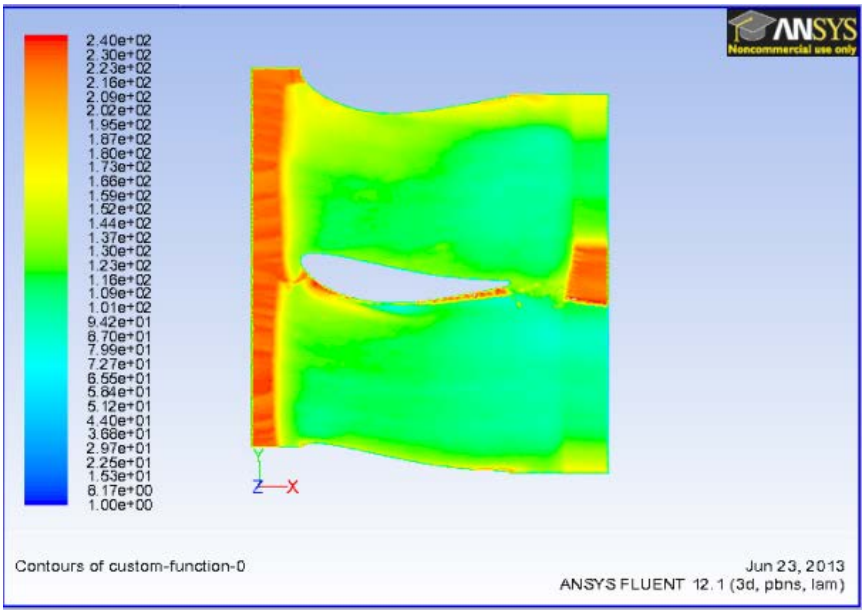

Figure 10.4: Convection heat transfer coefficient distribuiton

It is need to be mentioned that this pictures shows the values without the radiation correction. In order to repressent this variation, 4 graph are used. Each one represents one single row of the picture at a certain height. It can be seen in figure 10.5 the difference between the uncorrected (red) and corrected values (black).

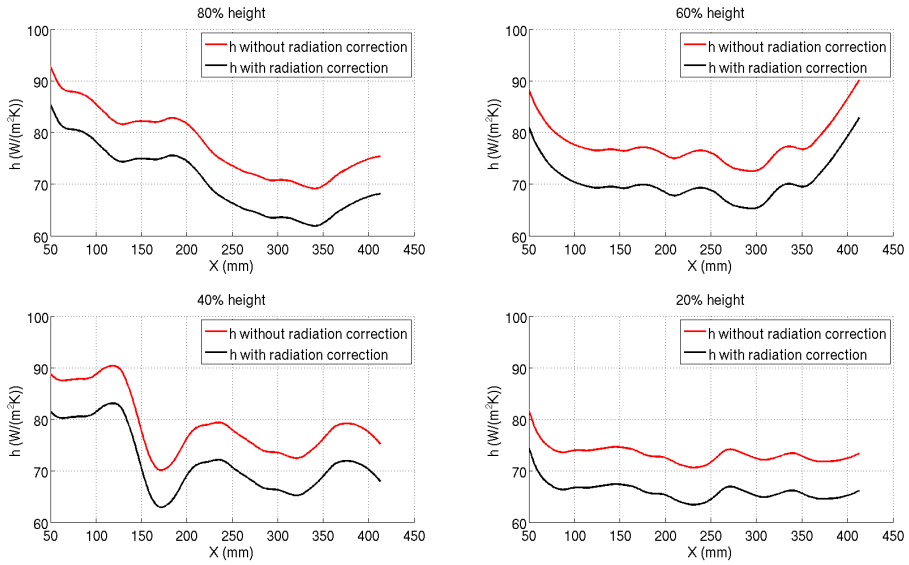

Figure 10.5: Radiation correction

10.3 Data precision

In every experiment there are many factors that can produce certain errors while obtaining the final data. In this case there are some aspects that contribute to have a certain amount of error. First of all, the tolerances of the manufactured parts of the experiment have to be taking into account. Then also the measurement devices like the infrared camera or the thermal resistors used in the experiment have a certain precision. For the camera the maximum temperature difference that can be detected is 0.01 ^oC and the RT100 measurement error is about 0.1. Another factor that can introduce errors during the measurements is the aperture of the window that could disturb the air flow and change the steady conditions.

In this experimkent the maximum precision obtained is about 0.01 degrees in terms of temperature and about 1mm in terms of space distribution due to the size of each pixel with a 10 per cent of estimated error.

Chapter 11

Conclusions

The main conclusion of this experiment is that the manufactured end wall complies with the requirements expected, working as it was planned. We can say then that using this method the convection heat transfer coefficient can be calculated properly with a certain grade of precision. So from this point many cases can be studied in the linear cascade changing the settups and flow conditions, which can provide us with deeper knowledge on this field and compare the data with other methods carried out previously.

Reffering to this experiment the convection heat transfer coefficient obtained is about 70 W/m^2K after the radiation correction. Also the areas with higher HTC values correspond to the interaction between the vane and the wall as it was expected. The boundary layer can be seen on the vane's profile, on the suction side.

Finally, due to timespands and manufacturing delays, the vane could not be studied. But everything is setted and prepared for running the experiment and get the data.

Bibliography

[1] M. Bovo, (2013) *"Single Pulse Jet Impingement on Inclined surface. Heat transfer and flow field"*, 11th International Conference on Engines Vehicles, Capri, Italy.

[2] C. Arroyo Osso, (2009) *"Aerothermal Inestigation of an Intermediate Duct"*, Thesis for the Degree of Doctor of Philosophy, Chalmers University of Technology

[3] B.M. Rojo Perez, (2012) *"Experimental Heat Transfer Study in Intermediate Turbine Duct"*, Masters thesis in Solid Fluid Mechanics, Chalmers University of Technology

[4] Incropera, DeWitt, Bergman, Lavine (2007) *"Fundamentals of Heat and Mass Transfer"*, 6^{th} edition.

[5] J.P Holman, *"Heat Transfer"*, 10^{th} edition, McGraw Hill

[6] A.Kassab, E. Divo, J. Heidmann, E. Steinthorsson, F. Rodriguez, (2003) *"BEM/FVM conjugate heat transfer analysis of a three-dimensional film cooled turbin blades"*, International Journal of Numerical Methods for Heat and Fluid Flow, Vol. 13 lss: 5, pp.581 - 610

[7] $Phoenix^{TM}$ Camera System With RTIE. Version 120. Indigo Systems Corporation.